# Retrieving Atmospheric Temperature Profiles by Microwave Radiometry Using *a Priori* Information on Atmospheric Spatial-Temporal Evolution

Patrizia Basili, *Member, IEEE*, Stefania Bonafoni, Piero Ciotti, *Member, IEEE*, Frank Silvio Marzano, *Member, IEEE*, Giovanni d'Auria, and Nazzareno Pierdicca

***Abstract*—A new approach is presented to determine atmospheric temperature profiles by combining measurements coming from different sources and taking into account evolution models derived by conventional meteorological observations. Using a historical database of atmospheric parameters and related microwave brightness temperatures, we have developed a data assimilation procedure based on the geostatistical Kriging method and the Kalman filtering suitable for processing satellite radiometric measurements available at each satellite pass, data of a ground-based radiometer, and temperature profiles from radiosondes released at specific times and locations. The Kalman filter technique and the geostatistical Kriging method as well as the principal component analysis have proved very powerful in exploiting climatological *a priori* information to build spatial and temporal evolution models of the atmospheric temperature field. The use of both historical radiosoundings (RAOBs) and a radiative transfer code allowed the estimation of the statistical parameters that appears in the models themselves (covariance and cross-covariance matrices, observation matrix, etc.). We have developed an algorithm, based on a Kalman filter supplemented with a Kriging geostatistical interpolator, that shows a significant improvement of accuracy in vertical profile estimations with respect to the results of a standard Kalman filter when applied to real satellite radiometric data.**

***Index Terms*—Atmospheric remote sensing, geostatistical Kriging method, Kalman filtering, microwave radiometry.**

## I. Introduction

MICROWAVE radiometers, both from ground and satellite platforms, have been used for many years for profiling atmospheric parameters such as temperature, water vapor, and cloud liquid [1]–[6]. Unfortunately, radiometric retrievals of profiles suffer of inadequate vertical resolution and relatively poor accuracy, particularly when considering the region of sounding far from the sensor. Therefore, the results obtained from radiometric measurements by using standard retrieval algorithms, as multivariate linear regressions, do not always meet the requirements of meteorological applications. This is due to the insufficient information gathered by multifrequency or multiangle measurements and to the ill-posed nature of the inverse problem [7]. The difficulties are even increased by the unknown variations of the atmospheric conditions that occur as a function of both time and geographical location.

A successful way to overcome these problems is to increase the amount of information brought by measurements, by combining diverse kinds of available observations, including data collected by conventional meteorological networks. It is also convenient to take benefit of the accessible *a priori* information to be exploited within suitable retrieval algorithms.

In this paper, we present a new approach to retrieve atmospheric temperature profiles from microwave radiometric measurements taking into account temporal and spatial atmospheric evolution models derived by means of conventional meteorological observations.

We have used an available archive of atmospheric profiles from radiosounding observations (RAOBs) distributed all over the Italian territory. From this data set we inferred time and space correlations of the atmospheric temperature field that provided us with *a priori* information to be exploited in the retrieval process.

The database of microwave brightness temperatures needed for implementing the retrieval algorithm was computed from RAOBs by means of the Liebe's model [8]. It has been used to simulate observations from the special sensor microwave/temperature (SSM/T1) on board the Defence Meteorological Satellite Program (DMSP) platforms, in addition to ground-based observations at two water sensing channels (23.8 and 31.65 GHz) and three temperature sensing channels within the 60 GHz $O_2$ absorption complex (53.85, 55.45, and 57.97 GHz).

We have developed a retrieval algorithm based on a Kalman filter [9] supplemented with a Kriging geostatistical interpolator [10], suitable for processing different sources of measurements, such as ground-based radiometers, satellite measurements available at each satellite pass, and temperature profiles from radiosondes released at specific times and locations. Besides the Kalman filter algorithm implemented with a time evolution model, the Kriging geostatistical method has been used for developing a space evolution model of the temperature field under observation. Moreover, the principal component analysis

Manuscript received April 3, 2000; revised November 6, 2000. This work was supported in part by the Italian Space Agency (ASI), MURST, and the National Plan for Researches in Antarctica.

P. Basili and S. Bonafoni are with the Dipartimento di Ingegneria Elettronica e dell'Informazione, University of Perugia, 06125 Perugia, Italy (e-mail: basili@diei.unipg.it; bonafoni@diei.unipg.it).

P. Ciotti and F. S. Marzano are with the Dipartimento di Ingegneria Elettrica, University of L'Aquila, L'Aquila, Italy (e-mail: p.ciotti@ing.univaq.it; marzano@ing.univaq.it).

G. d'Auria and N. Pierdicca are with the Dipartimento di Ingegneria Elettronica, University of Roma "La Sapienza," 00184 Roma, Italy (e-mail: dauria@die.ing.uniroma1.it; mauro@die.ing.uniroma1.it).

Publisher Item Identifier S 0196-2892(01)07624-0.

[11] has been applied to the vertical profiles for summarizing the correlation of temperature at different altitude levels and dealing with a limited number of parameters.

Hereafter, we resume the content of the paper. In Section II we develop time and space evolution models in terms of transition matrices, able to project profiles among RAOBs times and locations. In Section III, with regard to the spatial evolution, we consider a geostatistical data assimilation procedure, namely the Kriging approach, that allows us to produce temperature profiles at locations where RAOBs are not available. Section IV is mainly concerned with the design of the retrieval algorithms. Besides a conventional time recursive Kalman filter, we consider a new algorithm based on a Kalman filter modified with Kriging interpolation, taking profit of information coming from the assimilation of RAOBs released at nearby stations. In Section V we present an application of the algorithms to SSM/T1 data and, finally, in Section VI, we draw some conclusions and make some comments on future developments of the work.

## II. Analysis of Temporal and Spatial Correlations of the Atmospheric Temperature Field

The knowledge of the temporal and spatial correlations of profiles can be very useful when retrieving the atmospheric temperature field from microwave data. In order to assess the relevance of such *a priori* information [12], we have performed a study based on historical RAOBs, to develop simple evolution models of the atmosphere, that is assumed to be a first order auto-regressive system. These models are also the source of the first guess, needed in the implementation of the statistical retrieval algorithms.

In this section, we verify the time as well as the space predictability of temperature profiles by means of discrete evolution models, represented by transition matrices. The temperature field is described by the function $t(x, y, z, \tau)$ of point $(x, y, z)$ and time $\tau$.

The data set used in this analysis consists of RAOBs released at six Italian stations (Rome: RM, Milan: MI, Udine: UD, Brindisi: BR, Trapani: TP, Cagliari: CA), four times a day at 0000, 0600, 1200, and 1800 Greenwich Mean Time (GMT), from May to September for a total of ten years (from 1988 to 1997). From the original RAOBs after the application of quality control and interpolation procedures, profiles of $n = 84$ fixed altitude levels, representing the atmosphere from 0 to 27 km, have been produced and processed.

### A. Time Transition Matrix

In this study, a temporal autorecursive evolution model is developed for summer conditions at the six Italian stations, in terms of a transition matrix $\Phi_k$ of dimension $(n \times n)$ according to the expression

$$\mathbf{t}(k) = \Phi_k(k-1,\, k)\mathbf{t}(k-1) \tag{1}$$

where $\mathbf{t}$ is the vector of temperature profiles whose elements are the temperatures $t(x, y, z_l, \tau)$ at each of the $l = 1,84$ levels of the profiles, and indices $k-1$ and $k$ define two successive time instants. Since we consider radiosoundings separated by an interval of 6 h, we can build eight transition matrices to produce an estimate of the temperature profile at a specific time, given the profile measured 6 h before (forward transition) or 6 h later (backward transition). Moreover, it is possible to further improve the performances of the evolution model using a bidirectional transition. This is obtained by linearly combining the estimates of the forward and backward transition matrices using weights equal to the inverse of the projection error covariance matrices [13]

$$\mathbf{t}(k) = \left(\mathbf{S}_f^{-1} + \mathbf{S}_b^{-1}\right)^{-1}\Big[\mathbf{S}_f^{-1}\Phi_k(k-1,\, k)\mathbf{t}(k-1) + \mathbf{S}_b^{-1}\Phi_k(k+1,\, k)\mathbf{t}(k+1)\Big] \tag{2}$$

where $\Phi_k(k-1,\, k)$ and $\Phi_k(k+1,\, k)$ are the transition matrices, respectively, for the forward and backward transitions, with projection error covariance matrices $\mathbf{S}_f$ and $\mathbf{S}_b$.

For the computation of transition matrices $\Phi_k$, we have considered three approaches based on multivariate statistical techniques: the first two are the ordinary least squares (OLS) and the ridge least squares (RLS) regressions [14], while the third one is based on the principal component (PC) analysis [11]. Given m temperature profiles taken from the RAOB data base at a specified station and sounding time, let $\mathbf{T}_{k-1}$ and $\mathbf{T}_k$ be the $(n \times m)$ matrices whose columns are the temperature profile vectors $\mathbf{t}_{k-1}$ and $\mathbf{t}_k$, measured at sounding times $\tau_{k-1}$ and $\tau_k$, respectively. Considering a multivariate linear regression approach for (1), where $\mathbf{t}_{k-1}$ and $\mathbf{t}_k$ play the role of predictors and predictands respectively, the matrix of regression coefficients gives the transition matrix $\Phi_k$ and, for the first two mentioned regression methods, it is estimated by the following expressions:

$$\text{OLS:}\quad \Phi_k = \mathbf{T}_k\mathbf{T}_{k-1}^T\left(\mathbf{T}_{k-1}\mathbf{T}_{k-1}^T\right)^{-1} \tag{3}$$

$$\text{RLS:}\quad \Phi_k = \mathbf{T}_k\mathbf{T}_{k-1}^T\left(\mathbf{T}_{k-1}\mathbf{T}_{k-1}^T + \alpha\mathbf{I}\right)^{-1} \tag{4}$$

where

| | |
|---|---|
| superscript $T$ | matrix transposition; |
| $\mathbf{T}_{k-1}\mathbf{T}_{k-1}^T$ | estimate of the covariance matrix of $\mathbf{t}$ computed from the available data set at time $\tau_{k-1}$; |
| $\mathbf{T}_k\mathbf{T}_{k-1}^T$ | estimate of the cross-covariance matrix of $\mathbf{t}$ between times $\tau_k$ and $\tau_{k-1}$; |
| $\mathbf{I}$ | $(n \times n)$ identity matrix; |
| $\alpha$ | stabilizing positive constant chosen as discussed in [14]. |

The benefit of the RLS technique is relevant when the data set of predictors exhibits a high degree of colinearity. In the same case OLS may fit a training set very well but sometimes it gives less accurate results when applied to an independent test set.

For the third approach, we have preliminarly applied the Principal Component analysis by expanding the 84-level temperature profiles on a basis of empirical orthogonal functions (e.o.f.s) [15]. The PC technique permits a reduction of the number of descriptive profile parameters by exploiting the correlation among temperature values at different altitudes. Therefore, we can approximate each profile with a linear combination of a limited number of e.o.f.s. This reduction of state-space dimensionality allows one to diminish calculation

time and to improve the accuracy in estimating statistical quantities when only a limited set of training profiles is available in the historical data base.

The principal component analysis is performed by first computing the matrix $\mathbf{E}$ of eigenvectors (the e.o.f.s $\mathbf{e}$) of the covariance matrix $\mathbf{T}\mathbf{T}^T$ of vectors $\mathbf{t}$ and then determining each vector $\mathbf{p}$ of the principal components as

$$\mathbf{p} = \mathbf{E}^T\mathbf{t}. \tag{5}$$

The approximated reconstruction of a profile at each altitude $z_l$ is then obtained through the following equation:

$$t(z_l) \cong \sum_{j=1}^{r} p_j e_j(z_l); \qquad l = 1, n; r < n \tag{6}$$

where $e_j(z_l)$ is the element $l$ of the eigenvector $\mathbf{e}_j$ (the e.o.f. at elevation $z_l$) and the number $r$ of PCs is selected on the basis of a threshold on the desired reconstruction error (0.5 K RMS in our case).

Using this approach, we have considered a 12-element vector $\mathbf{p}$ of principal components of temperature profiles, instead of the 84-element vector $\mathbf{t}$ of temperatures, so that the transition matrix dimension is consequently reduced.

The transition matrix for the principal components $\Phi_k$ is then estimated by Ordinary least square regression (OLS-PC) according to the following equation:

$$\text{OLS-PC:} \quad \Phi_k = \mathbf{P}_k\mathbf{P}_{k-1}^T\left(\mathbf{P}_{k-1}\mathbf{P}_{k-1}^T\right)^{-1} \tag{7}$$

where $\mathbf{P}_{k-1}\mathbf{P}_{k-1}^T$ and $\mathbf{P}_k\mathbf{P}_{k-1}^T$ are the estimates of covariance and cross-covariance matrices of $\mathbf{p}$ computed from the available data set.

We have not considered the application of the RLS technique to the principal components of temperature profiles, because the PC technique employs a basis of empirical orthogonal functions and the PCs are uncorrelated variables, so the colinearity problem is overcome.

As an example, we show the application of the considered time evolution model to the RAOBs collected at Pratica di Mare, near Rome, and hereafter referred to as Rome RAOBs, where the training set for estimating the transition matrix contains $m = 1289$ RAOBs relative to the summer season (from May to September) during the years from 1988 to 1993 and 1995. Considering an independent set of 463 RAOBs from the same station and the same season, acquired in 1996, a comparison of the predicted profiles to the measured ones has been performed. By using the transition matrices computed by means of the three techniques described above, Table I reports the prediction accuracy in terms of vertically averaged root mean square (RMS) errors (i.e., averaged over all the 84 levels). The table contains results that consider the forward ($\rightarrow$), backward ($\leftarrow$) and bidirectional ($\rightarrow \leftarrow$) projections. The last row in the table is the vertically averaged climatological variability (i.e., the standard deviation of the temperature profile data set averaged over all the 84 levels). This table is related to the summer profile estimations in Rome, but the transition matrices have been also computed for the other stations, showing comparable accuracies of the time evolution models.

TABLE I
VERTICALLY AVERAGED ESTIMATION RMSEs [$K$] OF ATMOSPHERIC TEMPERATURE PROFILES IN ROME (TEST SET FROM MAY TO SEPTEMBER 1996) FOR TIME TRANSITION MATRICES COMPUTED USING THE THREE REGRESSION TECHNIQUES. RIGHT ARROW ($\rightarrow$) REPRESENTS THE FORWARD TRANSITION, LEFT ARROW ($\leftarrow$) THE BACKWARD TRANSITION, AND THE DOUBLE ARROW ($\rightarrow \leftarrow$) THE COMBINATION OF THE TWO TRANSITIONS BY THE INVERSE COVARIANCE MATRICES. THE LAST ROW REPORTS THE CLIMATOLOGICAL VARIABILITY OF THE DATA (CLIM) FOR THE PERIOD FROM MAY TO SEPTEMBER FROM 1988 TO 1993 AND 1995 TO 1996

| | h.00 | h.06 | h.12 | h.18 |
|---|---|---|---|---|
| OLS | $\rightarrow$ 1.82 | $\rightarrow$ 1.86 | $\rightarrow$ 1.91 | $\rightarrow$ 1.81 |
| | 2.08 $\leftarrow$ | 1.90 $\leftarrow$ | 1.76 $\leftarrow$ | 1.77 $\leftarrow$ |
| | $\rightarrow$ 1.79 $\leftarrow$ | $\rightarrow$ 1.57 $\leftarrow$ | $\rightarrow$ 1.56 $\leftarrow$ | $\rightarrow$ 1.48 $\leftarrow$ |
| RLS | $\rightarrow$ 1.52 | $\rightarrow$ 1.51 | $\rightarrow$ 1.56 | $\rightarrow$ 1.33 |
| | 1.73 $\leftarrow$ | 1.52 $\leftarrow$ | 1.46 $\leftarrow$ | 1.46 $\leftarrow$ |
| | $\rightarrow$ 1.50 $\leftarrow$ | $\rightarrow$ 1.32 $\leftarrow$ | $\rightarrow$ 1.32 $\leftarrow$ | $\rightarrow$ 1.23 $\leftarrow$ |
| OLS-PC | $\rightarrow$ 1.77 | $\rightarrow$ 1.76 | $\rightarrow$ 1.77 | $\rightarrow$ 1.49 |
| | 1.66 $\leftarrow$ | 1.93 $\leftarrow$ | 1.72 $\leftarrow$ | 1.54 $\leftarrow$ |
| | $\rightarrow$ 1.73 $\leftarrow$ | $\rightarrow$ 1.55 $\leftarrow$ | $\rightarrow$ 1.51 $\leftarrow$ | $\rightarrow$ 1.49 $\leftarrow$ |
| clim | 3.58 | 3.64 | 3.62 | 3.53 |

It can be observed that the best results are obtained by RLS regression, which decreases the RMS uncertainty from the climatological 3.6 K to about 1.5 K for both forward and backward transitions. Using the bidirectional transition, useful for off-line data re-analysis, the RMSE decreases further to about 1.3 K.

### *B. Space Transition Matrix*

Similarly to the temporal evolution, a spatial evolution model has been developed, still for summer conditions at the six Italian stations, in the form of a transition matrix $\Phi_s$ between couples of contemporaneous profiles at two stations

$$\mathbf{t}(r_j) = \Phi_s(r_i, r_j)\mathbf{t}(r_i) \tag{8}$$

where $\mathbf{t}(r_j)$ is the temperature profile vector at a specific RAOB station, given the profile $\mathbf{t}(r_i)$ measured at a different station, and $r_j$ and $r_i$ indicate the different locations $x_j$, $y_j$ and $x_i$, $y_i$. The transition matrix can be estimated as in the Section II-A, by OLS, RLS and OLS-PC techniques using formulas that correspond to (3), (4), and (7), respectively. Moreover, we can also estimate the temperature profile at each location by linearly combining the profiles estimated using the space evolution model from each of the other five stations, using again the weighted method with the inverse of the projection error covariance matrices, as in the following expression:

$$\mathbf{t}(r_j) = \left(\sum_{i=1}^{n_s} \mathbf{S}_{ij}^{-1}\right)^{-1}\left(\sum_{i=1}^{n_s} \mathbf{S}_{ij}^{-1}\Phi_s(r_i, r_j)\mathbf{t}(r_i)\right) \tag{9}$$

where here $n_s = 5$, $\Phi_s(r_i, r_j)$ is the transition matrix to a specific station $j$ from one of the other five stations, and $\mathbf{S}_{ij}$ is the projection error covariance matrix computed for the space evolution from the station $i$ to the fixed station $j$.

As an example, Table II reports the accuracy of spatial predictions in terms of vertically averaged RMSEs when using $\Phi_s$ matrices computed by the previously mentioned regression algorithms, for the RAOBs projected toward Rome from each of the

TABLE II
VERTICALLY-AVERAGED ESTIMATION RMS ERRORS [$K$] OF ATMOSPHERIC TEMPERATURE PROFILES PROJECTED TOWARD ROME FROM THE OTHER STATIONS (TEST SET FROM MAY TO AUGUST, 1996: 0000, 0600, 1200, 1800 GMT) FOR SPACE TRANSITION MATRICES COMPUTED USING THREE REGRESSION TECHNIQUES. THE LAST COLUMN DESCRIBES THE PREDICTION ERRORS USING THE INVERSE ERROR COVARIANCE WEIGHTED METHOD. THE LAST ROW REPORTS THE CLIM FOR EACH STATION FOR THE PERIOD FROM MAY TO SEPTEMBER 1988, 1990, 1995, AND 1996

| | MI –> RM | UD –> RM | BR –> RM | TP –> RM | CA –> RM | comb-cov |
|---|---|---|---|---|---|---|
| OLS | 2.15 | 2.01 | 1.92 | 1.89 | 2.14 | 1.59 |
| RLS | 2.02 | 1.92 | 1.85 | 1.83 | 1.95 | 1.56 |
| OLS_PC | 1.99 | 1.98 | 1.82 | 1.80 | 1.93 | 1.57 |
| clim | (MI) 3.73 | (UD) 3.64 | (BR) 3.52 | (TP) 3.32 | (CA) 3.62 | (RM) 3.59 |

other Italian stations. The results of the application of the projection method in (9) are reported in the last column (comb-cov). The climatological variability at each station for the summer season is also reported in the last row of the table. The table refers to the overall (i.e., vertically averaged) profile prediction error computed for a test set different from the training set used to infer the regression coefficients. The table is related to the summer profile estimations in Rome, but the transition matrices have been also computed for the other stations, showing comparable accuracies of the space evolution models.

Also in this case, the application of the evolution model decreases the climatological uncertainty and again the RLS technique gives always the best results. The combined covariance method (comb-cov) provides always predictions more accurate than those obtainable from single stations.

## III. ESTIMATING TEMPERATURE FIELD BY KRIGING INTERPOLATION

The combination of measurements performed at different times and locations is a typical task of the so-called data assimilation, that is the process of finding the model of the analyzed system most consistent with the observations in order to reach the best spatial and temporal resolutions [16]–[19].

The evolution models derived in the previous section suffer of the same resolution limits of the available RAOBs, that is they can perform projections only among RAOB locations and times. Also, satellite microwave radiometric measurements generally do not match RAOBs in space and time, thus preventing from directly using the mentioned models in the retrieval of temperature profiles. To overcome these limitations, we have used a basic tool of applied geostatistics, i.e., the Kriging interpolation, a powerful technique able to produce regularly sampled fields in the presence of non regularly spaced observations.

In this section, we formulate the basics of the Kriging method as applied to the problem of atmospheric temperature profiling, considering only horizontal correlations for simplicity of exposition. In our study, this is justified by the particular implementation based on the PC analysis, as described further on.

The Kriging method is a weighted moving average technique and gives an estimate as a weighted linear combination of the available sample values around the point to be evaluated. For each altitude $z_l$, with $l = 1,84$, the interpolated value of the sought temperature $t_l(\mathbf{r}_0) = t_l(x_0, y_0)$ at a generic location $\mathbf{r}_0$ is given by the following linear combination:

$$t_l(\mathbf{r}_0) = \sum_{i=1}^{q} w_{il} t_l(\mathbf{r}_i) \tag{10}$$

where $w_{il}$ are the weights for the values available at the $q$ sample data points $(\mathbf{r}_i,\ i = 1,\ q)$.

In our study the sample data points are the $q = 6$ Italian RAOB stations and the meteorological data set is provided by RAOBs released four times a day. The vector of weights is obtained by solving the system of the so called ordinary Kriging equations [10] and is given by

$$\mathbf{w} = \mathbf{C}^{-1}\mathbf{d} \tag{11}$$

where matrix $\mathbf{C}$ contains the temperature cross-covariances between RAOB stations, and vector $\mathbf{d}$ contains the unknown temperature cross-covariances between each station and the point to be predicted. To obtain the Kriging weights $\mathbf{w}$, we have carried out the classical two steps of the geostatistical process.

First, in the *descriptive analysis* step, for handling location dependent data, the extent of data correlation, or spatial continuity of the temperature field, is described through a structure function (the semivariance or covariance function) [20], [21]. The semivariance $\gamma(\mathbf{h})$ of the temperature field at each altitude level $z_l$ represented as a semivariogram, has the expression

$$\gamma_l(\mathbf{h}) = \frac{1}{2N(\mathbf{h})} \sum_{(i,j)|(\mathbf{r}_i - \mathbf{r}_j = \mathbf{h})} [t_l(\mathbf{r}_i) - t_l(\mathbf{r}_j)]^2 \tag{12}$$

where $t_l(\mathbf{r}_i) = t_l(x_i, y_i)$ and $t_l(\mathbf{r}_j) = t_l(x_j, y_j)$ are temperature values at altitude level $z_l$ for the two different sites $\mathbf{r}_i$ and $\mathbf{r}_j$, and $N(\mathbf{h})$ is the number of pairs of data whose locations are separated by a given displacement vector $\mathbf{h}$ in the horizontal plane, with components $h_x$, $h_y$. We have computed the empirical two-dimensional (2-D) semivariance for each altitude $z_l$, as expressed by (12). In our case, considering the six available RAOB stations, we have 15 possible pairs of sites, providing 15 different values of $\mathbf{h}$, and 15 samples of the empirical semivariogram. In the computations we have used $N(\mathbf{h}) = 211$ corresponding to the number of RAOB profiles available at the same times (summer of years 1988, 1990, 1995, 1996) from all the six stations. To give an idea of the temperature field in the horizontal plane, we have vertically averaged the experimental $\gamma(\mathbf{h})$ functions and we have represented in Fig. 1 the obtained mean semivariogram as a contour plot. The shape of the contour lines shows a temperature pattern anisotropy, i.e., a directional asymmetry of spatial continuity. From this empirical semivariogram it is possible to quantify the higher degree of correlation in the East–West direction and the shorter correlation length in the north–south direction.

In the subsequent *predictive application* step we have adopted, as suggested in [10], a parameterized exponential function for the cross-covariance matrix in (11), that is we have assumed

$$C_{ij} = C(\mathbf{r}_i - \mathbf{r}_j) = C(\mathbf{h}) = \sigma^2 \exp(-3h_A) \tag{13}$$

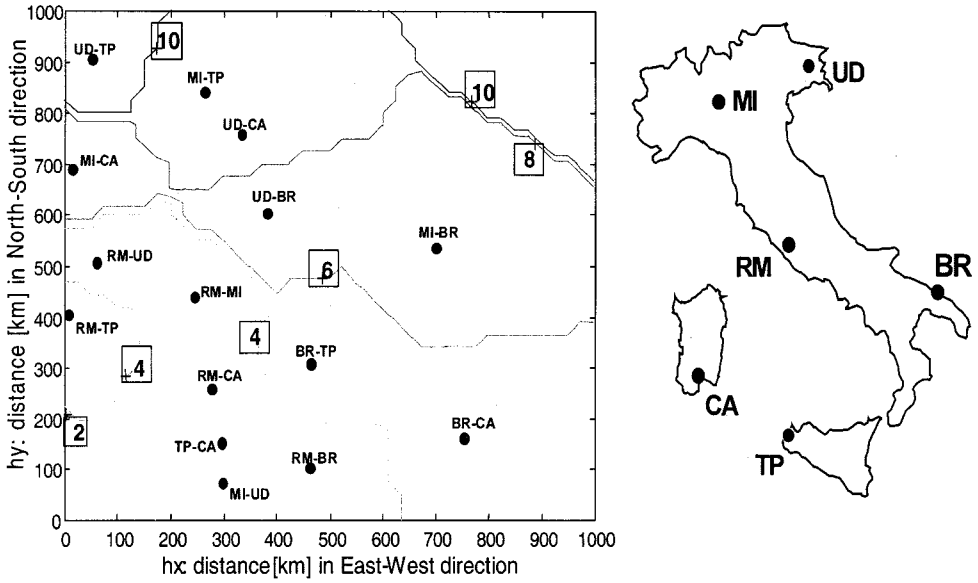


Fig. 1. Descriptive analysis results shown as a two-dimensional (2-D) empirical semivariogram contour-plot (left panel). Values $[K^2]$ are related to the vertically-averaged semivariance for the 15 pairs of stations. The right panel shows the non-regularly spaced locations of the RAOB stations.

where

$$h_A = \sqrt{\left(\frac{h_x}{a_x}\right)^2 + \left(\frac{h_y}{a_y}\right)^2}$$

$\sigma^2$ is the asymptotic semivariogram value (sill), representing the variance of the temperature at a certain altitude, and $\mathbf{a} = (a_x, a_y)$ is a vector representing the range (distance beyond which the semivariogram remains essentially constant) in the in east–west $(a_x)$ and north–south $(a_y)$ direction. In this 2–D model, a difference in range parameters accounts for the presence of possible anisotropy. Once the parameters have been determined by fitting the empirical semivariogram, all the terms of matrix $\mathbf{C}$ and vector $\mathbf{d}$ in (11) can be computed and the weights $w$ are therefore determined.

In our approach, the Kriging estimator has been applied to the principal components of temperature profiles, instead of the temperature fields at each RAOB level. The principal components can justify the choice of a 2-D semivariogram $\gamma(h_x, h_y)$. In fact the PCs are uncorrelated quantities and the associated e.o.f.s intrinsically contain the information about correlation along the altitude coordinate.

A study to tune the range parameters $a_x$ and $a_y$ of the assumed 2-D anisotropic model has been performed for our application of the Kriging interpolator to the first 12 principal components of temperature profiles. This study has shown that the best trade-off for all stations can be achieved by selecting $a_x \cong 3000$ km and $a_y \cong 2000$ km.

For the selected values of the range parameters, Fig. 2 shows the profiles of RMS interpolation error at each station. It is possible to note the reliable prediction of the Kriging technique and the reduction of uncertainty for all stations compared to the climatological RMS. Hence, Kriging interpolator can be considered an efficient tool for building an evolution model able to overcome spatial sampling limitations.

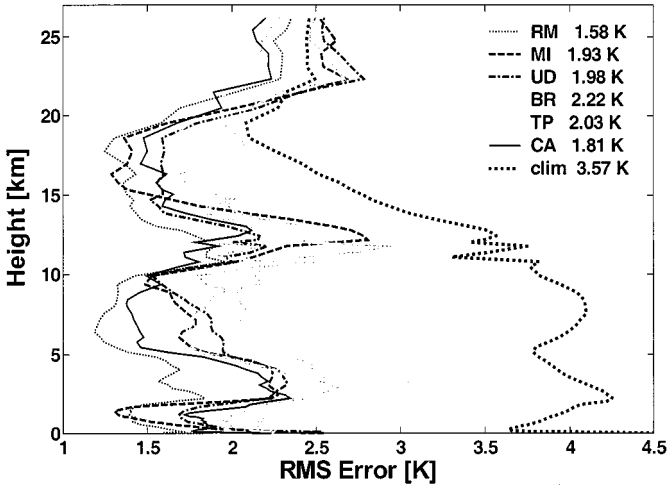


Fig. 2. Cross-validation results in terms of interpolation RMSE profiles for each station, using 12 principal components and $a_x = 3000$ km and $a_y = 2000$ km, compared to climatological variability for test RAOBs from May to September of the years 1988, 1990, 1995, 1996. In the legend vertically-averaged RMSEs $[K]$ are reported.

## IV. Inversion by Kalman Filter

In many retrieval problems, the optimal combination of measurements, which become available as time progresses, can be approached from a Bayesian standpoint, leading to the derivation of the Kalman filter equations [9], [22], [23].

### A. Standard Kalman Filter

The use of Kalman filtering in the microwave radiometric retrieval of atmospheric temperature profiles has been already discussed elsewhere [24]–[27]. In the following text, only a brief description of the relevant equations will be given.

It is assumed that the atmosphere is a linear, stochastic dynamical system, and the radiometric measurements are consid-

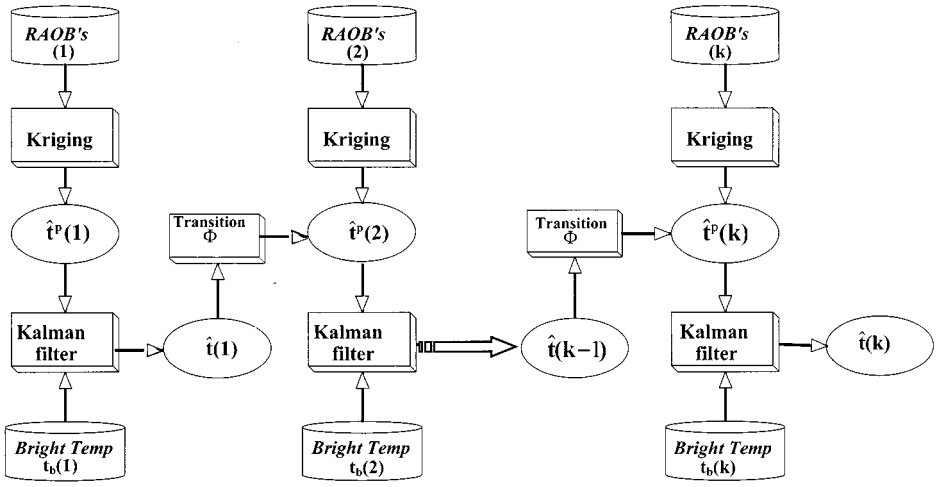


Fig. 3. Modified Kalman filter block diagram.

ered to be linearly related to the state vector (i.e., the temperature profile vector) through the following expression:

$$\mathbf{t_B} = \mathbf{W}\mathbf{t} + \mathbf{n} \tag{14}$$

where

- $\mathbf{t_B}$ measurement vector (i.e., the brightness temperatures at different frequencies or observation angles);
- $\mathbf{t}$ state vector;
- $\mathbf{n}$ measurements noise;
- $\mathbf{W}$ observation matrix (i.e., the matrix of the discrete temperature weighting functions).

Note that in the following equations we use the caret to indicate the estimate, superscript $p$ to represent the *a priori* expectation, and the arguments $k-1$ and $k$ to define two successive instants $\tau_k$ and $\tau_{k-1}$.

The Kalman linear estimation algorithm produces an unbiased, minimum variance estimate $\hat{\mathbf{t}}(k)$ of temperature at time $\tau_k$ given the current measurement vector $\mathbf{t}_B(k)$, as in the following expression:

$$\hat{\mathbf{t}}(k) = \hat{\mathbf{t}}^p(k) + \mathbf{K}(k)\left[\mathbf{t_B}(k) - \mathbf{W}(k)\hat{\mathbf{t}}^p(k)\right] \tag{15}$$

where $\hat{\mathbf{t}}^p(k)$ is the *a priori* temperature profile considered at the current time, and the Kalman gain $\mathbf{K}(k)$ is defined by

$$\mathbf{K}(k) = \mathbf{C}^p_{\mathbf{tt}}(k)\mathbf{W}^T(k)\left[\mathbf{W}(k)\mathbf{C}^p_{\mathbf{tt}}(k)\mathbf{W}^T(k) + \mathbf{R}(k)\right]^{-1} \tag{16}$$

where $\mathbf{R}(k)$ is the covariance matrix of the measurement error $\mathbf{n}$ and $\mathbf{C}^p_{\mathbf{tt}}(k)$ is the covariance matrix of the error on the *a priori* predicted profile. The *a priori* profile at time $\tau_k$ is obtained from the estimated profile at time $\tau_{k-1}$ using the following recursive scheme:

$$\hat{\mathbf{t}}^p(k) = \mathbf{\Phi}_k(k-1, k)\hat{\mathbf{t}}(k-1) \tag{17}$$

where $\Phi_k$ is the time transition matrix already introduced in Section II. In (16), the error covariance matrix $\mathbf{C}^p_{\mathbf{tt}}$ of the *a priori* predicted profile to be used in the computation of the Kalman gain at time $\tau_k$ can be projected from the *a posteriori* error covariance matrix $\mathbf{C_{tt}}$ at time $\tau_{k-1}$ using the following equation:

$$\mathbf{C}^p_{\mathbf{tt}}(k) = \mathbf{\Phi}_k(k-1, k)\mathbf{C_{tt}}(k-1)\mathbf{\Phi}^T_k(k-1, k) + \mathbf{Q}(k-1) \tag{18}$$

where $\mathbf{Q}$ is the plant noise matrix representing the covariance of a random additive error in the time transition model (17). The accuracy of the estimate (15) is quantified by its *a posteriori* error covariance matrix

$$\mathbf{C_{tt}}(k) = [\mathbf{I} - \mathbf{K}(k)\mathbf{W}(k)]\mathbf{C}^p_{\mathbf{tt}}(k). \tag{19}$$

At the first step (for $k = 1$), the recursive procedure of the filter is initialized by using in (15) the best available *a priori* estimate of the temperature profile, usually obtained from the climatological mean profile.

### *B. Kalman Filter with Kriging Interpolation*

Unfortunately, the implementation of the standard Kalman filter suffers of the already mentioned lack of matching between the locations of the radiometric observations (i.e., the measurement vector $\mathbf{t}_B$) and those of RAOBs, that provide the *a priori* information, the related statistics, and the transition matrices.

To overcome this limitation, a new retrieval algorithm has been designed for recovering temperature profiles in sites without historical climatological knowledge. It is a Kalman filter modified with an interpolation based on the Kriging method, and its block diagram is shown in Fig. 3. The *a priori* information to be applied in the first step of the Kalman algorithm is provided by Kriging interpolation of contemporary profiles measured at the available RAOB stations, instead of the climatological mean profile. For the successive steps, we apply the recursive scheme of the Kalman algorithm using the time evolution model summarized by the transition matrix $\Phi_k$ but taking also profit of the information coming from the Kriging interpolation of RAOBs available at each time step.

As shown in the block diagram, the classical filtering (15) and (16) are preserved, but the *a priori* profile is now an inverse covariance weighted average of the Kalman *a posteriori* estimate of the previous step projected through matrix $\Phi_k$ and the

Kriging interpolated profile $\mathbf{t}_{\text{int}}$ (computed following the procedure developed in the previous section), as expressed by the following combination:

$$\hat{\mathbf{t}}^P(k) = \left(\mathbf{S}_{\text{trans}}^{-1} + \mathbf{S}_{\text{int}}^{-1}\right)^{-1} \cdot \left[\mathbf{S}_{\text{trans}}^{-1}\boldsymbol{\Phi}_k(k-1,\, k)\hat{\mathbf{t}}(k-1) + \mathbf{S}_{\text{int}}^{-1}\mathbf{t}_{\text{int}}(k)\right] \tag{20}$$

where

$$\mathbf{S}_{\text{trans}} = \boldsymbol{\Phi}_k(k-1,\, k)\mathbf{C}_{\mathbf{tt}}(k-1)\boldsymbol{\Phi}_k^T(k-1,\, k) + \mathbf{Q}(k-1) \tag{21}$$

is the covariance matrix of the error related to the temporal transition of the standard Kalman filter, and $\mathbf{S}_{\text{int}}$ is the covariance matrix of the error related to the spatial Kriging interpolation. The particular formulation of the *a priori* estimate (20), following the reference [13], leads to an error covariance matrix $\mathbf{C}_{\mathbf{tt}}^p(k)$ to be used in the computation of the Kalman gain, modified according to the following expression:

$$\mathbf{C}_{\mathbf{tt}}^p(k) = \left\{\left[\boldsymbol{\Phi}_k(k-1,\, k)\mathbf{C}_{\mathbf{tt}}(k-1)\boldsymbol{\Phi}_k^T(k-1,\, k) + \mathbf{Q}(k-1)\right]^{-1} + \mathbf{S}_{\text{int}}^{-1}\right\}^{-1}. \tag{22}$$

In this procedure, to which we will refer in the following as the modified Kalman filter, the time transition matrices $\Phi_k$ as well as the observation matrices $\mathbf{W}$ for locations without historical climatological knowledge are computed by using the Kriging interpolation approach so that this modified Kalman algorithm allows the processing of radiometric observations gathered in any geographical site.

## V. Application to Satellite (SSM/T1) and Ground-Based Radiometric Data

The algorithm described in the previous section has been applied to DMSP SSM/T1 data with the additional contribution of simulated ground-based radiometric data.

The SSM/T1 is a seven channel microwave radiometer designed to provide global, synoptic scale soundings of temperature throughout the troposphere and lower stratosphere. The seven frequency channels are located in the oxygen band at 50.50, 53.20, 54.35, 54.90, 58.40, 58.825, and 59.40 GHz [28]. The SSM/T1 is a cross-track nadir scanning radiometer having, at the nominal 833 km altitude, a nadir circular footprint with a diameter of 175 km; the antenna reflector is rotated to seven scan positions separated by 12° with a maximum cross-track scan angle of 36°. Typical instrument noise levels are on the order of 0.5 K RMS or less. More complete details can be found in [29].

In our retrievals we have used the SSM/T1 passes over Italy close to the secondary synoptic hours, i.e., almost contemporary to the RAOB acquisition times at 0600 and 1800 GMT. We have not made use of the two channels at lower frequencies because of the Earth surface influence, which is not easily predictable due to the large sensor footprint and to the variable characteristics of the Italian area. To sense the lower part of the atmosphere the satellite measurements can be combined with data of a ground-based radiometer [30]. The ground-based brightness temperatures have been simulated at two water vapor and liquid sensing channels (23.8 and 31.65 GHz), and at three temperature sensing channels within the 60 GHz oxygen band (53.85, 55.45, and 57.97 GHz). The mentioned frequencies correspond to the channels of a ground based radiometer that will be very soon installed in an experimental site located in Central Italy. As ancillary measurement, we consider also the atmospheric temperature measured at the surface.

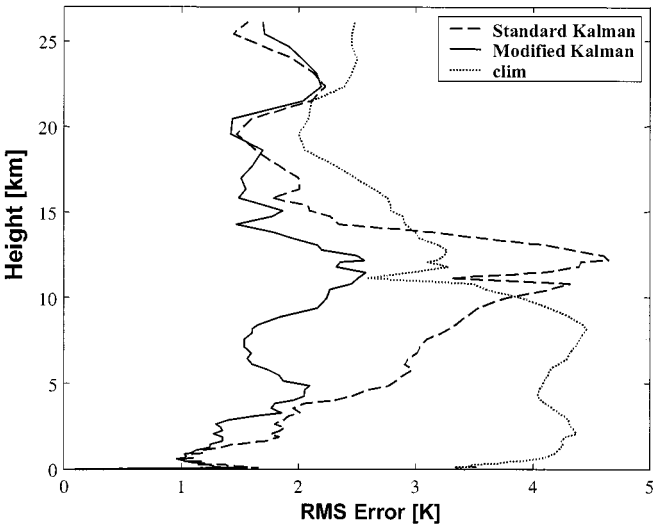


Fig. 4. RMSE profiles for a set of 32 test RAOBs in Rome (from June 1, 1997 to June 22, 1997) applying the first step of the Kalman filter. The dashed line is the standard Kalman filter error, the continuous line is the modified (i.e., using Kriging interpolation) Kalman filter estimation error, both without the temporal transition model. The climatological variability (dotted line) is representative of the period from May to September of the years 1988, 1990, 1995, and 1996.

The aim of the experimental effort was to asses the performances of the modified Kalman filter using Kriging interpolation, by comparing the retrieved temperature profiles to RAOBs. We have performed the validation considering a location where the RAOBs were available, specifically the site of Rome. Of course, the Rome RAOBs have never been used in the development of the inversion algorithm, but only for evaluating the retrieval errors. Hereafter we present retrieval results, obtained by applying the inversion algorithm sketched in Fig. 3 to combined data (real satellite and synthetic ground-based radiometric data). We have compared different implementations of the retrieval algorithm in order to appraise the relative contributions of introducing spatial and temporal *a priori* information in the procedure.

In the beginning, for evaluating the spatial contribution, we consider both standard and modified Kalman filter approaches stopped at the first step, that is implementations that do not include the time evolution model. As for the modified Kalman filter the space Kriging interpolated profile is used as first guess, instead of the simple mean temperature profile (climatological), that is used for the standard approach.

Concerning this first step of the Kalman filter approaches, in Fig. 4 the profiles of RMSEs computed from a set of 32 SSM/T1 measurements, collected in June 1997 over Rome, are shown superimposed to the corresponding climatological RMS profile (dotted line). The dashed line refers to the standard Kalman estimation error, while the continuous line refers to the modified Kalman estimation error. The corresponding vertically averaged error is 2.24 K using the standard Kalman approach and it is reduced to 1.62 K when the modified Kalman approach is used.

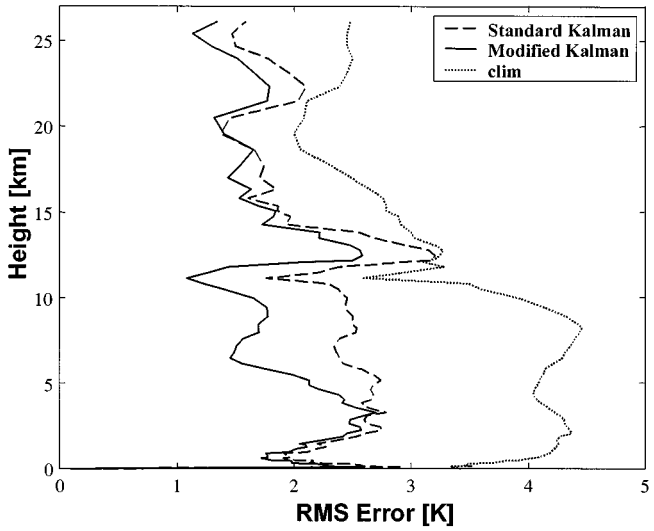


Fig. 5. Comparison of RMSE profiles for a set of 32 test RAOBs in Rome (from June 1, 1997 to June 22, 1997) obtained by standard Kalman filter (dashed line) and modified Kalman filter using Kriging interpolation (continuous line), both incorporating the temporal transition model. The climatological variability (dotted lines) is representative of the period from May to September of the years 1988, 1990, 1995, and 1996.

This should be compared to the 3.59 K climatological standard deviation of the entire database.

The interpolated profile used in the modified Kalman approach appears more consistent with the real state of the atmosphere with respect to the pure climatological first guess, since it exploits the contemporary temperature field of the nearby stations and therefore contributes to improve the Kalman filter performance.

Then, for evaluating also the contribution of temporal *a priori* information, we show an example of application of the complete Kalman approaches employing also the time evolution model. The RMSE profiles, derived from the same SSM/T1 case of Fig. 4, are plotted in Fig. 5. Again, the dotted line is the climatological RMS. The figure shows the results of a standard Kalman filter (dashed line) that does not account for spatial interpolation, and the estimation accuracy obtained by the modified Kalman filter based on the Kriging method (continuous line). The corresponding overall vertically averaged RMSEs are 1.94 K and 1.47 K, respectively, against a climatological RMSE of 3.59 K.

The comparison among the results of Figs. 4 and 5 points out the contribution of the temporal evolution model, included in the complete recursive Kalman algorithms, both in the standard and modified version. By comparing the RMS of the standard to the modified Kalman approach, it is also evident the significant improvement of the performances when the Kriging interpolations are injected in the procedure.

From the results shown in this section it can be noted the relevance of the *a priori* information brought by the Kriging interpolation and the good performance of the Kalman filtering in the combination of any *a priori* information with measurements. In particular, the modified Kalman filter shows a substantial reduction of the uncertainty of the climatological. first guess, exploiting simultaneous nearby temperature profiles. Thus, the recursive scheme with time evolution model, applied to sequences of radiometric measurements, takes benefit in the estimation process from the improved and more reliable first guess.

## VI. Conclusions

The combination of spatial and temporal evolution models of the three-dimensional (3-D) field of atmospheric temperature has been proved very useful for improving the final accuracy of temperature profile retrieval by spaceborne and ground based microwave radiometers. The Kalman filter technique and the geostatistical Kriging method together with the principal component analysis have been proved very powerful in exploiting the *a priori* information.

The computation of empirical time evolution model for the temperature profiles (at RAOB sites) has been used for implementing a Kalman filter able to process sequences of satellite and ground-based radiometric measurements.

The use of the Kriging interpolation has allowed the development of a modified Kalman filter, capable of processing also radiometric observations collected at geographical sites without historical climatological knowledge. We have performed a validation of the algorithm at a specific RAOB site, but the method is able to produce profiles at any generic location and to generate maps of temperatures at selected levels within the satellite swath.

We have achieved a significant improvement of accuracy in vertical profile estimations using real satellite radiometric measurements and atmospheric temperature measured at the surface. The contribution of a ground-based radiometer to improve the accuracy near the Earth surface has been included using simulated data, but future experimental campaigns with a ground-based instrument are already planned.

Even if, from an operational point of view, a drawback of the method can be represented by the difficulty in collecting data from different sources (conventional meteorological networks, satellite, ground radiometric sites), the exploitation of temporal and spatial correlations has proved very fruitful and can be adapted to different situations thanks to the flexibility of the proposed methodology.

## References

[1] D. C. Hogg, M. T. Decker, F. O. Guiraud, K. B. Earnshaw, D. A. Merrit, K. P. Moran, W. B. Sweezy, E. R. Westwater, and C. G. Little, "An automatic profiler of the temperature, wind, and humidity of the troposphere," *J. Climate Appl. Meteorol.*, vol. 22, pp. 807–831, 1983.

[2] J. I. H. Askne and E. R. Westwater, "A review of ground-based remote sensing of temperature and moisture by passive microwave radiometers," *IEEE Trans. Geosci. Remote Sensing*, vol. GE-24, pp. 340–352, 1986.

[3] J. W. Waters, F. K. Kunzi, R. L. Pettyjohn, and D. H. Staelin, "Remote sensing of atmospheric temperature profiles with the Nimbus 5 microwave spectrometer," *J. Atmos. Sci.*, vol. 32, pp. 1953–1969, 1975.

[4] A. V. Troitsky, K. P. Gajkovich, V. D. Gromov, E. N. Kadygrov, and A. Kosov, "Thermal sounding of the atmospheric boundary layer in the oxygen absorption band center at 60 GHz," *IEEE Trans. Geosci. Remote Sensing*, vol. 31, pp. 116–119, Jan. 1993.

[5] F. Del Frate and G. Schiavon, "Nonlinear principal component analysis for the radiometric inversion of atmospheric profiles by using neural networks," *IEEE Trans. Geosci. Remote Sensing*, vol. 37, pp. 2335–2342, Nov. 1999.

[6] S. J. English, "Estimation of temperature and humidity profile information from microwave radiances over different surface types," *J. Appl. Meteorol.*, vol. 38, pp. 1526–1541, 1999.

[7] E. R. Westwater and O. N. Strand, "Statistical information content of radiation measurements used in indirect sensing," *J. Atmos. Sci.*, vol. 27, pp. 960–967, 1970.

[8] H. Liebe, "MPM—An atmospheric millimeter-wave propagation model," *Int. J. IR & MM Wave*, vol. 10, pp. 631–650, 1989.

[9] A. Gelb, *Applied Optimal Estimation.* Cambridge: MIT Press, 1974.

[10] E. H. Isaaks and R. M. Srivastava, *An Introduction to Applied Geostatistics*. New York: Oxford Univ. Press, 1989.
[11] W. W. Cooley and P. R. Lohnes, *Multivariate Data Analysis*. New York: Wiley, 1971.
[12] P. Basili, S. Bonafoni, P. Ciotti, G. d'Auria, F. S. Marzano, and N. Pierdicca, "The role of *a priori* information in designing retrieval algorithms for radiometric profiling of the atmosphere," in *Proc. Int. Geoscience and Remote Sensing Symp.'97*, Singapore, 1997, pp. 2087–2089.
[13] C. D. Rodgers, "Retrieval of atmospheric temperature and composition from remote sensing measurements of thermal radiation," *Rev. Geophys. Space Phys.*, no. 4, pp. 609–624, Nov. 1976.
[14] L. J. Crone, L. M. Mc Millin, and D. S. Crosby, "Constrained regression in satellite meteorology," *J. Appl. Meteorol.*, vol. 35, pp. 2023–2035, Nov. 1996.
[15] W. L. Smith and H. M. Woolf, "The use of eigenvectors of statistical covariance matrices for interpreting satellite sounding radiometer observations," *J. Atmos. Sci.*, vol. 33, pp. 1127–1140, 1976.
[16] A. C. Lorenc, "Atmospheric data assimilation," U.K. Meteorol. Office, Forecasting Res. Div., Sci. Paper 34, May 1995.
[17] N. A. C. Cressie, *Statistics for Spatial Data*. New York: Wiley, 1993.
[18] D. G. Krige, "A statistical approach to some basic mine valuation problems on the Witwatersrand," *J. Chem., Metallurg. Mining Soc. South Africa*, vol. 52, pp. 119–139, 1951.
[19] G. Matheron, "Traité de geostatistique appliquée, Tome II: le Krigeage," in *Memoire du Bureau de Recherches Geologiques et Minieres*. Paris, France: Editions Bureau de Recherches Geologiques et Minieres, 1963.
[20] ——, "Principles of geostatistics," *Econ. Geol.*, vol. 58, pp. 1246–1266, 1963.
[21] Z. Sen, "Cumulative semivariogram models of regionalized variables," *Math. Geol.*, vol. 21, pp. 891–903, 1989.
[22] K. Brammer and G. K. Siffling, *Kalman–Bucy Filters*. Norwood, MA: Artech House, 1989.
[23] G. Noriega and S. Pasupathy, "Application of Kalman filtering to real-time preprocessing of geophysical data," *IEEE Trans. Geosci. Remote Sensing*, vol. 30, pp. 897–909, May 1992.
[24] W. H. Ledsham and D. H. Staelin, "An extended Kalman–Bucy filter for atmospheric temperature profile retrieval with a passive microwave sounder," *J. Appl. Meteorol.*, vol. 17, pp. 1023–1033, 1978.
[25] P. Basili, P. Ciotti, and D. Solimini, "Inversion of ground-based radiometric data by Kalman filtering," *Radio Sci.*, vol. 16, pp. 83–91, 1981.
[26] E. R. Westwater, J. B. Snider, and A. V. Carlson, "Experimental determination of temperature profiles by ground-based microwave radiometry," *J. Appl. Meteorol.*, vol. 14, pp. 524–539, 1975.
[27] P. Basili, S. Bonafoni, P. Ciotti, F. S. Marzano, G. d'Auria, and N. Pierdicca, "The use of time correlation in designing algorithms for microwave retrieval of atmospheric temperature profiles," *Atti della Fondazione Giorgio Ronchi*, vol. 54, pp. 483–493, 1999.
[28] H. E. Fleming, N. C. Grody, and E. J. Kratz, "The forward problem and corrections for the SSM/T satellite microwave temperature sounder," *IEEE Trans. Geosci. Remote Sensing*, vol. 29, pp. 571–583, May 1991.
[29] N. C. Grody, D. G. Gray, C. S. Novak, J. S. Prasad, M. Piepgass, and C. A. Dean, "Temperature soundings from the DMSP microwave sounder," *Adv. Remote Sensing Retrieval Methods*, 1985.
[30] E. R. Westwater, Z. Wang, N. C. Grody, and L. M. McMillin, "Remote sensing of temperature profiles from a combination of observation from the satellite-based microwave sounding unit and the ground-based profiler," *J. Atmos. Ocean. Technol.*, vol. 2, pp. 97–109, 1985.

**Patrizia Basili** (M'97) was born in Rome, Italy, on March 17, 1947. She received the Laurea degree in electronic engineering from the University of Rome, Rome, Italy, in 1972.

In 1973, she joined the Department of Electronic Engineering, University of Rome, were she taught courses on electromagnetic fields. She is now a Professor with the Institute of Electronics, University of Perugia, Perugia, Italy, and teaches a course on remote sensing and another on electromagnetic fields. She has also taught courses on electromagnetic wave theory while with Calabria University, Calabria, Italy, in 1977, and antennas and propagation while with Ancona University, Ancona, Italy, from 1978 to 1980. Her research activity has been concerned with microwave and millimeter-wave propagation in the atmosphere, atmospheric remote sensing by radiometry and inverse problems in electromagnetics.

**Stefania Bonafoni** was born in Fabriano, Italy, on March 9, 1971. She received the Laurea degree (cum laude) from the University of Perugia, Perugia, Italy, in 1997 and 2000, respectively, both in electronic engineering.

She is currently a Contract Researcher with the University of Perugia, teaching a course on electromagnetic fields at the DUIT, University of Perugia. Her research activity has been concerned with microwave and millimeter-wave propagation in the atmosphere, atmospheric remote sensing by radiometry, and inversion methods in electromagnetics.

**Piero Ciotti** (M'94) was borne in Rome, Italy, on November 10, 1952. He received the Laurea degree in electronic engineering (cum laude) from the University of Rome, Rome, Italy, in 1977.

He is currently a Professor of electromagnetics with the Department of Electrical Engineering, University of L'Aquila, L'Aquila, Italy, and was an Associate Professor with the University "La Sapienza," Rome, Italy, teaching a course on remote sensing before this. From 1984 to 1985, he conducted research at the NOAA/ERL Wave Propagation Laboratory, Boulder, CO, working on microwave radiometry applications to atmospheric remote sensing. He has been Principal Investigator within the MAESTRO radar polarimetric experiment and a Member of the ERS-1 Radar Altimeter calibration team. He is Principal Investigator in the ENVISAT project and member of the RA2/MWR, MERIS, MIPAS, GOMOS, and SCIAMACHY validation teams. His research activity has been concerned with microwave remote sensing of the environment, microwave and millimeter-wave propagation in the atmosphere, inverse electromagnetic problems, and digital signal processing.

**Frank Silvio Marzano** (S'89–M'99) received the Laurea degree (cum laude) in electronic engineering and the Ph.D. degree in applied electromagnetics, both from the University "La Sapienza," Rome, Italy, in 1988 and 1993, respectively.

In 1993, he collaborated with the Institute of Atmospheric Physics, Consiglio Nazionale Richerche (CNR), Rome, Italy. From 1994 to 1996, he was with the Italian Space Agency, Rome, Italy, as a Postdoctoral Researcher. After being a Lecturer at the University of Perugia, Perugia, Italy, in 1997, he joined the Department of Electrical Engineering, University of L'Aquila, L'Aquila, Italy, where he presently holds the position of Assistant Professor. His current research concerns passive and active remote sensing of the atmosphere from ground-based, airborne, and spaceborne platforms, with a particular focus on precipitation using microwave and infrared data, development of inversion methods, radiative transfer modeling of scattering media, and scintillation and rain-fading analysis along satellite microwave links.

Dr. Marzano received the Young Scientist Award of the XXIV General Assembly of the International Union of Radio Science (URSI) in 1993. In 1998, he was the recipient of the Alan Berman Publication Award (ARPAD) from the Naval Research Laboratory, Washington, DC.

**Giovanni d'Auria** was born in Rome, Italy, on June 23, 1931. He received the degree in electrical engineering and the Lib.Doc. degree, both from the University "La Sapienza," Rome, Rome, Italy in 1956 and 1964, respectively. He was with the Italian Air Force, working in ITAV Laboratories, Rome, from 1957 to 1968. He then was with Fondazione Ugo Bordoni as a Researcher in the Antennas and Propagation Laboratory, Rome, from 1959 to 1962. In 1962, he joined the University of Rome, Department of Electronics, as an Assistant Professor, teaching applied electronics. In 1976, he was appointed Professor in the Chair of Antennas and Propagation and has been teaching this subject since then. His current research concerns electromagnetic propagation in a turbulent atmosphere, microwave remote sensing of the atmosphere and Earth's surface, and microwave radiometry of the atmosphere (particularly of cloud systems).

**Nazzareno Pierdicca** received the Laurea degree in electronic engineering (cum laude) from the University "La Sapienza," Rome, Italy, in 1981.

From 1978 to 1982, he was with the Italian Agency for Alternative Energy (ENEA), Casaccia, Rome. From 1982 to 1990, he was with Telespazio, Rome, in the Remote Sensing Division. He was involved in various projects concerning remote sensing applications, data interpretation, and ground segment design. He was Principal Investigator of the ESA/JRC Agrisar '86 airborne campaign in 1986 and Co-Investigator of the X-SAR/SIR-C Experiment. In November 1990, he joined the Department of Electronic Engineering "La Sapienza" University. His research activity mainly concerns electromagnetic scattering model, microwave radiometry of the atmosphere, and SAR applications to vegetation. He is Investigator of the MAC Europe '91 and X-SAR/SIR-C experiments. He is presently an Associate Professor and teaches remote sensing at the Faculty of Engineering, University "La Sapienza."